INVESTIGATION OF OSB THICKNESS-SWELL BASED ON A 3-D DENSITY DISTRIBUTION. PART II. VARIATIONS IN THICKNESS-SWELL AND INTERNAL STRESSES

Alan D. Tackie

Engineer
OPUS Architects and Engineers
10350 Bren Road
West Minnetonka, MN 55343

Siqun Wang†

Associate Professor
Tennessee Forest Products Center
The University of Tennessee
2506 Jacob Dr
Knoxville, TN 37996-4563

Richard M. Bennett

Professor
221 Perkins Hall
Department of Civil and Environmental Engineering
The University of Tennessee
Knoxville, TN 37996-2010

(Received June 2006)

Abstract. A recently developed finite element (FE) model was used to examine the thickness-swell, density changes, and internal stresses in oriented strandboard (OSB) panels under moisture loading. The model accounts for the nonlinear mechanical behavior of OSB and for the moisture transport through the specimen. The FE model is based on the 3-D density variation of the board. The density variation, resulting from manufacturing processes, affects the uniformity of thickness-swell in OSB and is often exacerbated by continuous sorption of moisture, which leads to potentially damaging internal stresses in the panel. The model was validated through comparison of experimental results. The use of the model is illustrated by quantifying the effects of resin content changes on thickness swell, and the examination of internal stresses and bond failures in an OSB specimen.

Keywords: Thickness-swell, oriented strandboard, modeling, density distribution, resin content, finite element.

INTRODUCTION

Oriented strandboard (OSB) is a complex wood composite that has nonuniform density distribution in both the through-the-thickness (vertical) direction and in the in-plane (horizontal) direction (Wang and Winistorfer 2000). The three-dimensional (3-D) density distribution affects many properties of the panel performance, such as stiffness, strength, and thickness-swell. A nonuniform density distribution results in the development of internal stresses in the panel as the panel undergoes moisture changes (Van Houts et al 2004, 2006). Locations in the panel with higher density will tend to swell more than areas with lower density. The differential swelling causes internal stresses to develop perpendicular to the surface of the panel. Compressive stresses will develop in locations of higher potential

* Corresponding Author: swang@utk.edu
† SWST Member

swell as the swell is being restrained. Tension stresses will develop in locations of lower potential swell as the panel is being stretched. If the tensile stresses are great enough, there can be internal failures in the panel, resulting in delaminations.

Suchsland (1962) was one of the first to recognize this problem, stating that variations in the horizontal density are undesirable because differential swelling between areas of varying density could cause damaging internal stresses in a panel. Linville (2000) used a simple mechanics model to examine values of internal stresses based on horizontal density variations. Recently, the authors (Tackie et al 2008) developed a FE model that predicts thickness-swell based on the 3-D density distribution, accounting not only for horizontal density variations, but also for vertical density variations. The purpose of this paper is to apply the developed FE model to predict internal stresses, and illustrate the use of the finite elements for modeling the behavior of OSB.

MATERIALS AND METHODS

Two southern pine (*Pinus spp*.) commercial OSB panels were used in this work. The panels were chosen based on the results of previous tests to have very different average thickness-swells. Test specimens, 150 × 150 × 18 mm, were cut from the panels. The test specimens had an initial average moisture content of 2%, determined through oven-drying. The assumed resin type for these commercially obtained OSB specimens was diphenyl methane diisocyanate (MDI). The soak test adopted followed ASTM D1037−06 standards for evaluating thickness swell for wood composites (ASTM 2006). The specimens, first coated on the bottom surface with a silicone water sealant, were permitted to dry over a 24-h period. The four edges and top surface were left unsealed to reflect modeling conditions. Thickness-swell measurements were made at times of 2, 4, 8, 16, and 24 h.

Density distributions in the plane of test specimens, HDD, and distributions through-the-thickness of the specimens, VDP, were obtained with the aid of an X-ray densitometer. Attenuation data were collected at 400 points/m. At a nominal thickness of 18 mm, seven data points were collected at 3-mm intervals through-the-thickness of the specimens. Details of the determination of the 3-D density distribution from the data are in Tackie et al (2008).

THE FINITE ELEMENT MODEL

A FE model was developed to predict the thickness-swell of OSB panels based on the 3-D density distribution. The element used linear interpolation functions and had degrees-of-freedom only in the out-of-plane (through-the-thickness) direction. A nonlinear modulus of elasticity (MOE) was used, being a function of density, moisture content, and resin content. Empirical equations developed by Linville (2000) were used for the MOE. The unsteady-state moisture transfer equation developed by Cloutier et al (2001) for wood composites was used to model the moisture flow in the OSB panel. The transverse diffusion coefficient, as given by Cloutier et al (2001), is a function of the porosity of the wood, the average moisture content between nodes, the temperature, and the density. Details of the FE model are in Tackie (2006).

To model the 150- × 150- × 18-mm test specimens, 12 elements were used in the length and width directions, and 6 elements were used through-the-thickness. This created 7 nodal planes through-the-thickness, with the nodal planes being numbered from the bottom (sealed surface) to the top (unsealed surface). The results of the measured and predicted average thickness-swell are shown in Fig 1. The model was able to capture both the 24-h average thickness-swell and the moisture diffusion through time.

RESULTS AND DISCUSSION

The FE model enables variations in thickness-swell, density, and internal stresses to be examined, giving a much better understanding of the behavior of OSB than just average thickness-swell. For example, 3-D plots of nodal-planes 7

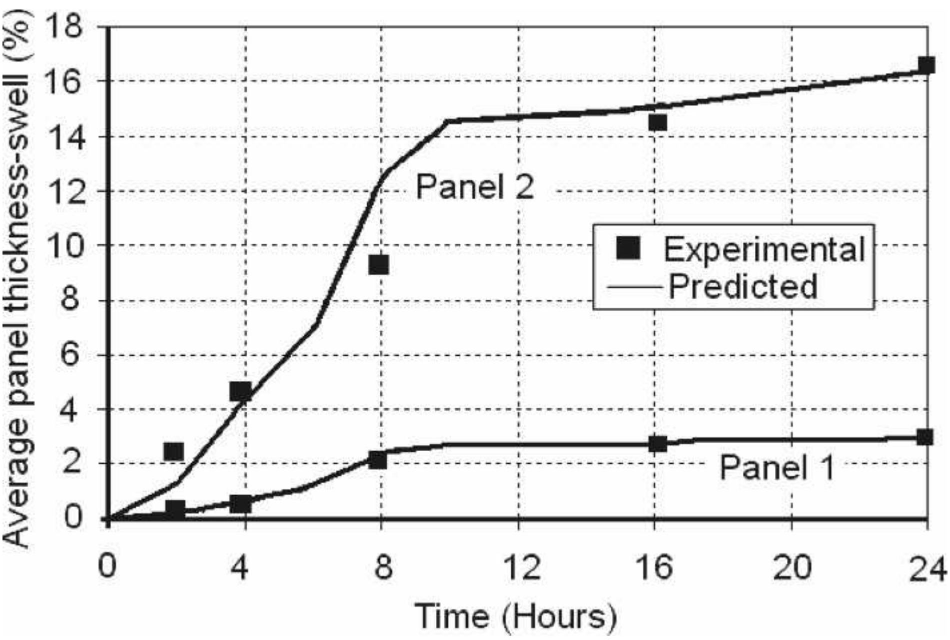

FIGURE 1. Measured and predicted average thickness-swell.

(top), 4 (middle), and 2 (bottom) thickness-swell distributions after 24-h soak time are shown in Fig 2 for specimen 1. The strand orientations of nodal-planes 7 and 2 are along the panel length and are perpendicular to nodal-plane 4, where they are oriented along the panel width. Thickness-swell was relatively higher at the corners than at the midsection of the specimen. Unlike nodes in the interior portion of a specimen, nodes at the corners are unrestrained along two edges and free to swell or translate in the thickness direction. Model predictions of excessive swell at the corners were consistent with experimental measurements.

The thickness swell can be related to the density distribution. Figures 3 and 4 show the initial top nodal-plane density distribution and the predicted density distribution after 24-h soak time. The initial density in the top nodal plane ranged 380–820 kg/m^3 with an average of 590 kg/m^3. After 24-h soak time, the nodal-plane density ranged 370–560 kg/m^3 with an average of 470 kg/m^3, or a 21% decrease. Figure 5 shows the change in top nodal-plane density after 24-h water soak.

The behavior along nodal-lines 6 and 10 parallel to the length was compared. The average initial density was 620 kg/m^3 for nodal-line 6 and 590 kg/m^3 for nodal-line 10. In other words, line 6 was a line of higher density and line 10 was one of lower density. After 24-h soak time, the average density along nodal-line 6 was 550 kg/m^3, an 11% decrease, and the average density along nodal-line 10 was 420 kg/m^3, a 29% decrease. Higher thickness-swell along nodal-line 10 was due to a combination of initial lower density, and from the proximity of line 10 to the edge where nodes are less constrained.

The behavior of specimen 1 can be compared with specimen 2, which had a much higher average thickness-swell. Figure 6 shows the top layer thickness-swell at different points in time. Not only is the average thickness-swell for specimen 2 greater than for specimen 1, but there is a much greater variation in thickness-swell. Figure 7 shows the density variation of specimen 2 after 24-h water soak. Density deviations from the mean specimen density were computed for all nodes and an overall coefficient of variation (CV) was used to quantify the den-

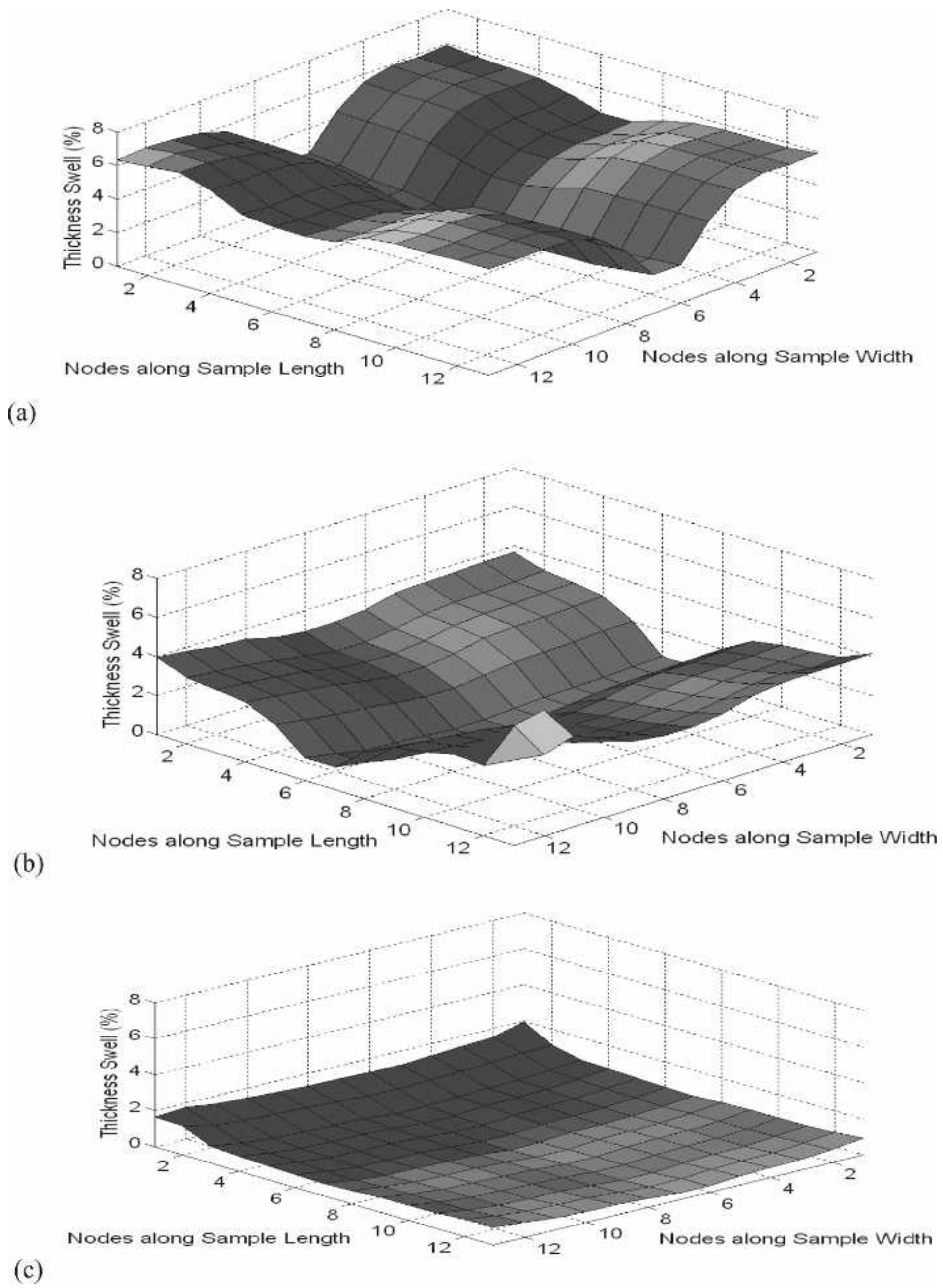

FIGURE 2. Thickness-swell for specimen 1 at 24 h: (a) nodal-plane 7, top (b) nodal-plane 4, middle (c) nodal-plane 2, bottom.

sity variation. Initially, the two specimens had similar variation, being 0.5% for specimen 1, and 0.6% for specimen 2. After a 24-h soak period there was still a relatively small density variation in specimen 1 (0.7%). However, specimen 2 had a 30% density variation. Specimen 2 not only had a large average thickness-swell, but also a highly variable thickness-swell.

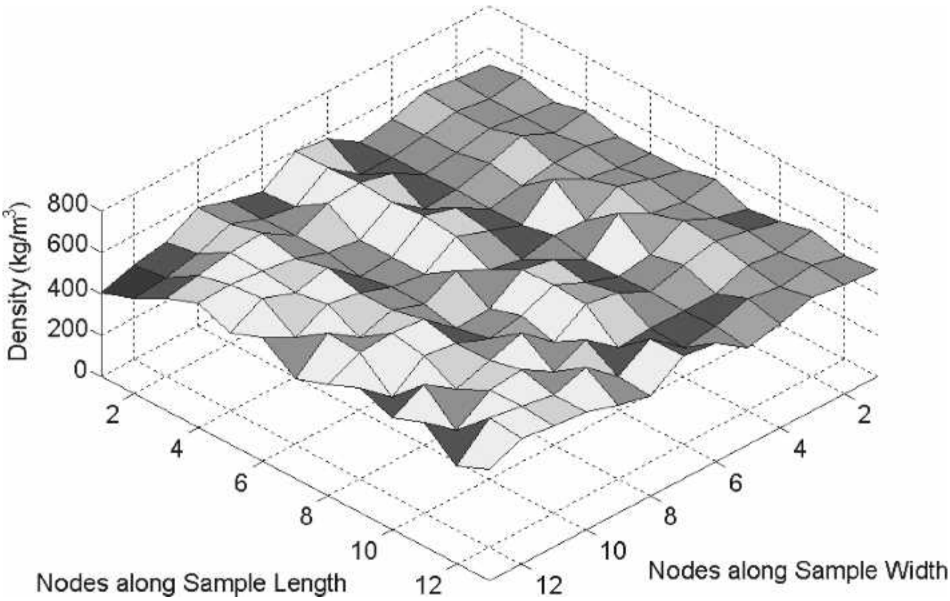

FIGURE 3. Initial top nodal-plane density distribution.

Density variations in an OSB panel, especially in the horizontal directions, cause differential swelling. The density variations cause regions of low density to resist the greater swelling in the surrounding high-density portions. The resistance induces stresses in the panel, which can cause bond-line failure. Tension will be induced in the low-density regions and compression in the high-density regions. The FE model is used to predict the internal stresses. Figure 8 shows a

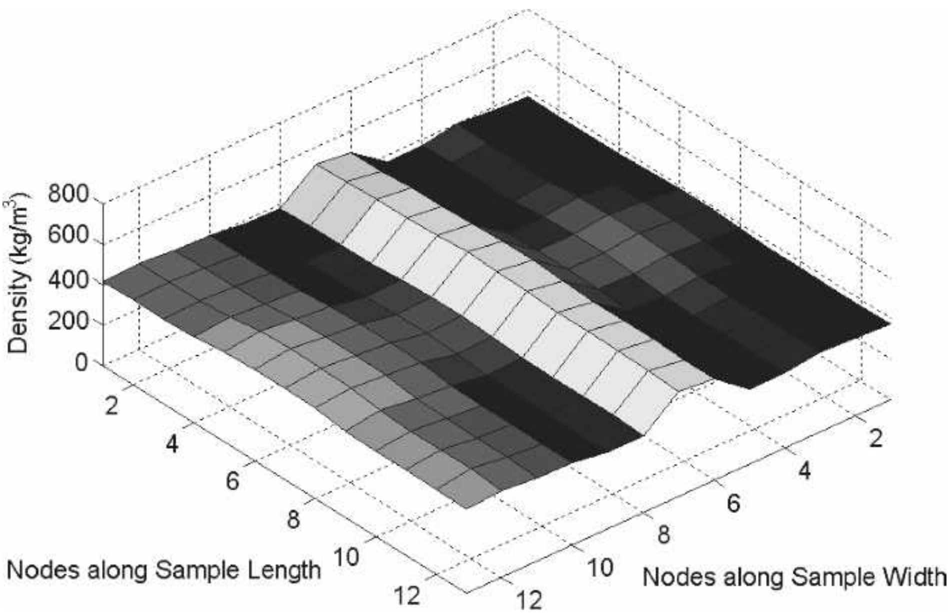

FIGURE 4. Top nodal-plane density distribution after 24-h soak.

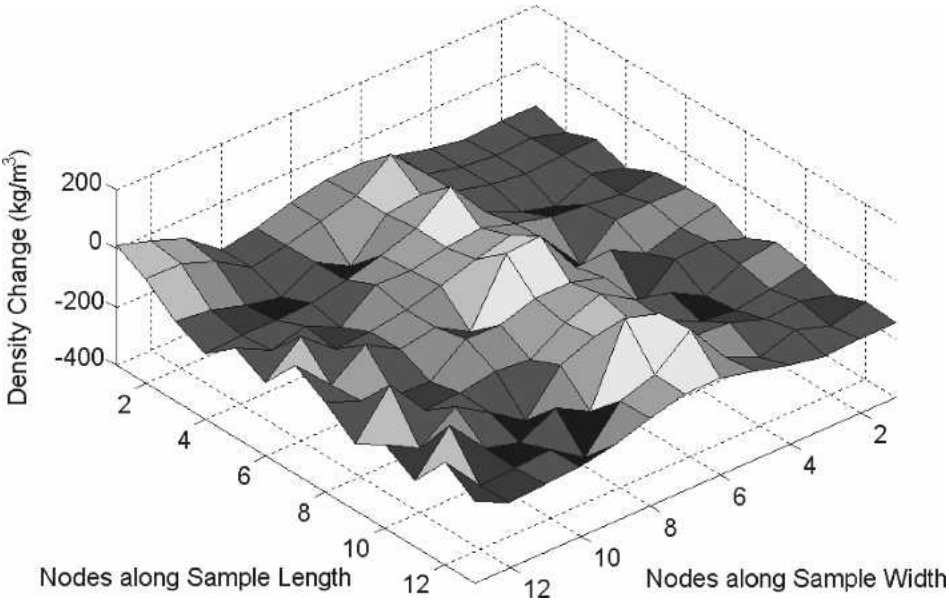

FIGURE 5. Top nodal-plane change in density after 24-h soak.

stress distribution plot of nodal-plane 4 of specimen 2, which had a greater variation in density. Compression stresses along nodal-line 6 in the length direction correspond to high-density regions (Fig 7(b)). The lower density at the edges results in tensile stresses in those regions.

Whenever tension stresses due to moisture loading exceed the internal bond, there is failure in the fabric of the panel. Linville (2000), in a similar study of failed panel fractions, developed an empirical equation for the internal bond strength, σ_{ult}, as a function of density, resin fraction, and moisture content, Eq (1).

$$\sigma_{u/t} = -229 + 0.823\rho + 165R - 24.8M \text{ (kPa)} \quad (1)$$

Where:

ρ = Density (kg/m^3)
R = Resin content (%)
M = Moisture content (%)

For specimen 2, with an average nodal-plane density of 310 kg/m^{3}after 24-h soak, average moisture content at fiber saturation point of 30%, and resin fraction of 5%, the ultimate strength evaluated using Eq (1), was 107 kPa. This estimate of ultimate strength indicated that most nodes in the plane have failed, especially along the edges of the nodal plane. This trend is in good agreement with observations made of OSB edge swell (Gu et al 2005; Wang and Winistorfer 2003) and with those observed in the experimental portion of this work.

Resin content effect on thickness-swell is well documented (Brochmann et al 2002; Wu and Lee 2002; Zhang et al 2007). Linville (2000) reported a decrease in thickness-swell with increasing resin fraction. For this case study, specimen 2 was selected due to its high thickness-swell. It was established through model calibration that the resin content of the experimental specimen was 5%. Experimentally determined and model predictions of thickness-swell were 16.9 and 16%, respectively. Using the developed model and keeping all other parameters constant, the resin fraction varied from 4 to 12%. Figure 9 shows thickness-swell as a function of percentage resin content. The down-sloping trend in thickness-swell as resin content increased, is in agreement with studies done by Linville (2000). In related research, Wu and Lee

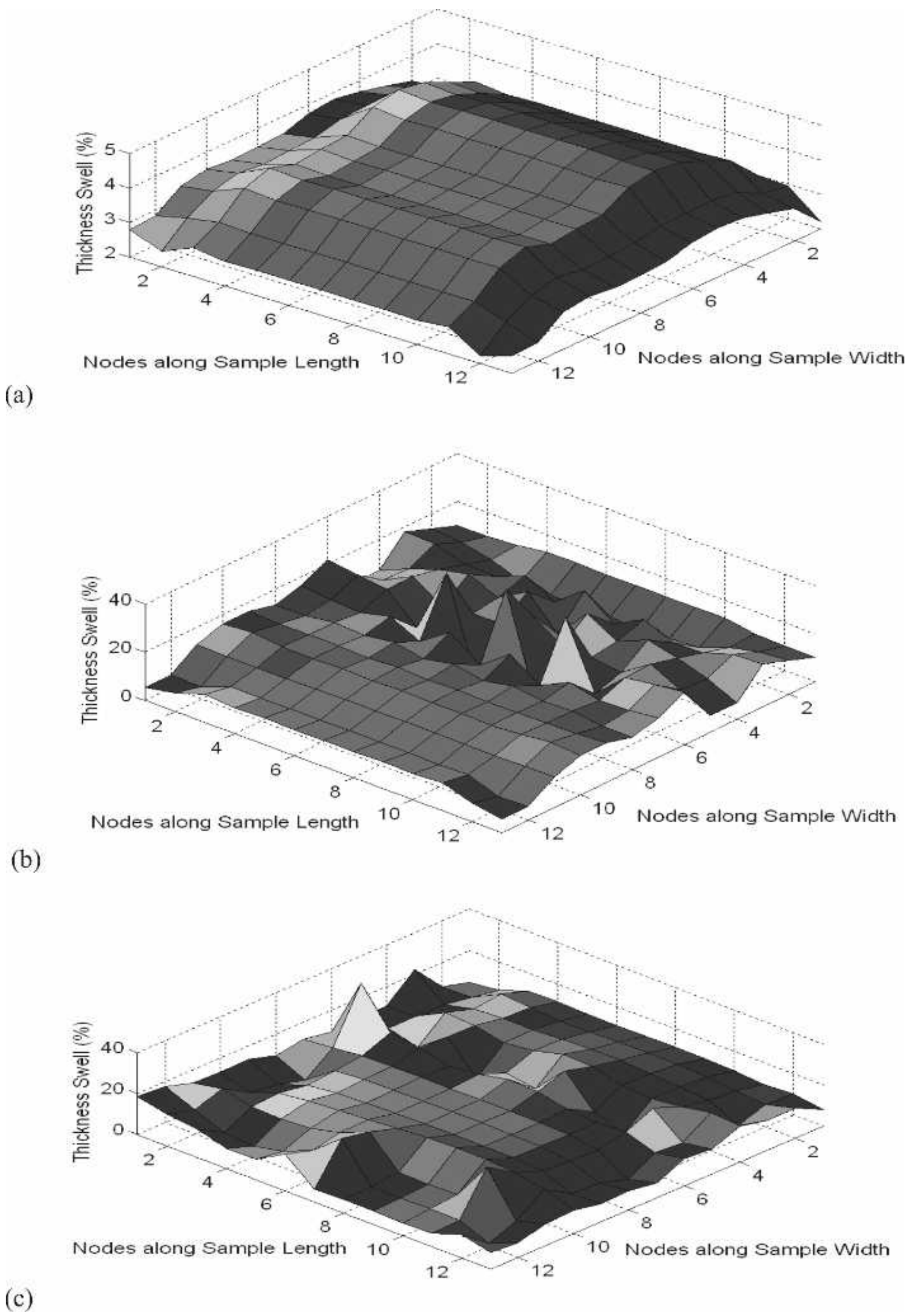

FIGURE 6. Top nodal-plane thickness-swell for specimen 2 at (a) 2 h (b) 12 h (c) 24 h.

(2002) also reported decreasing thickness-swell when resin fractions increased from 4 to 6%. As resin content decreased, variation in thickness-swell over the panel increased as well as total thickness swell. The FE model enables the quantitative improvement in panel performance to be

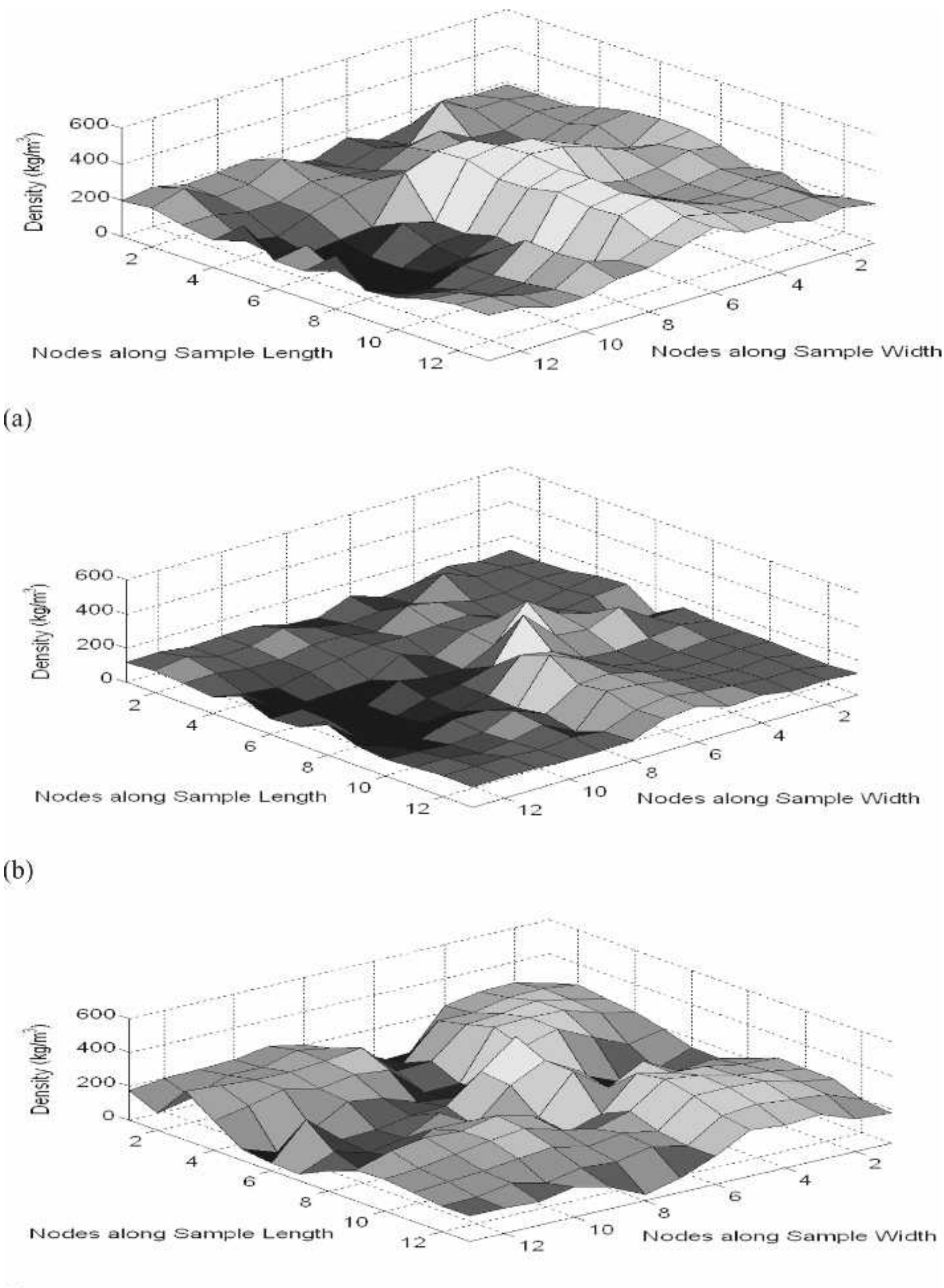

FIGURE 7. Density distributions for specimen 2 at 24 h: (a) nodal-plane 7, top (b) nodal-plane 4, middle (c) nodal-plane 2, bottom.

determined with increased resin content. An increase in resin content to 7% causes approximately a 50% decrease in average thickness-swell.

Model simulations of 2, 4, and 6% resin content were performed for specimen 2 while keeping other factors constant. A node was classified as failed if the imposed stress from moisture load-

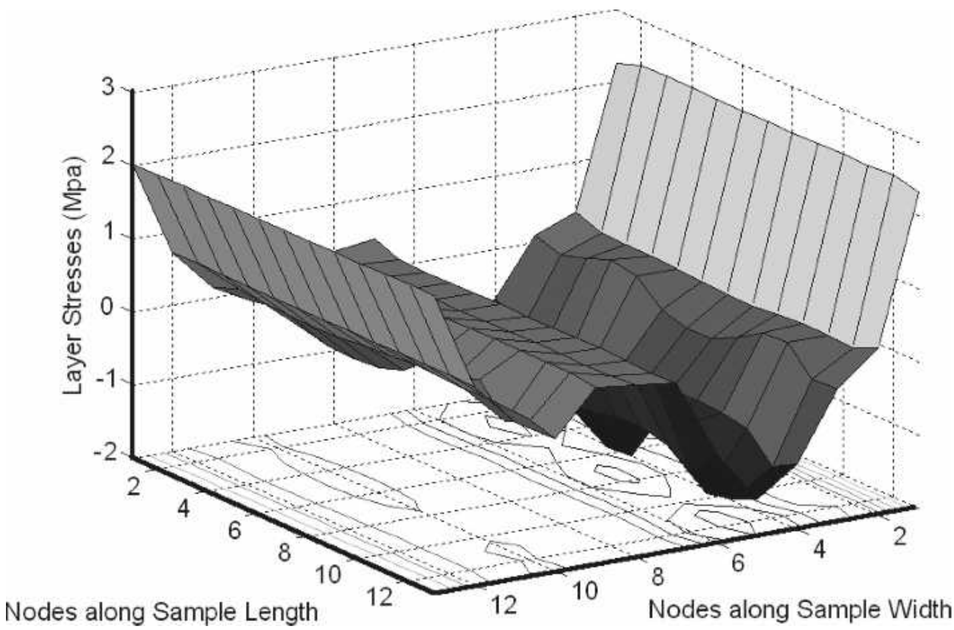

FIGURE 8. Specimen 2 nodal-plane 4 stress distribution after 24 h.

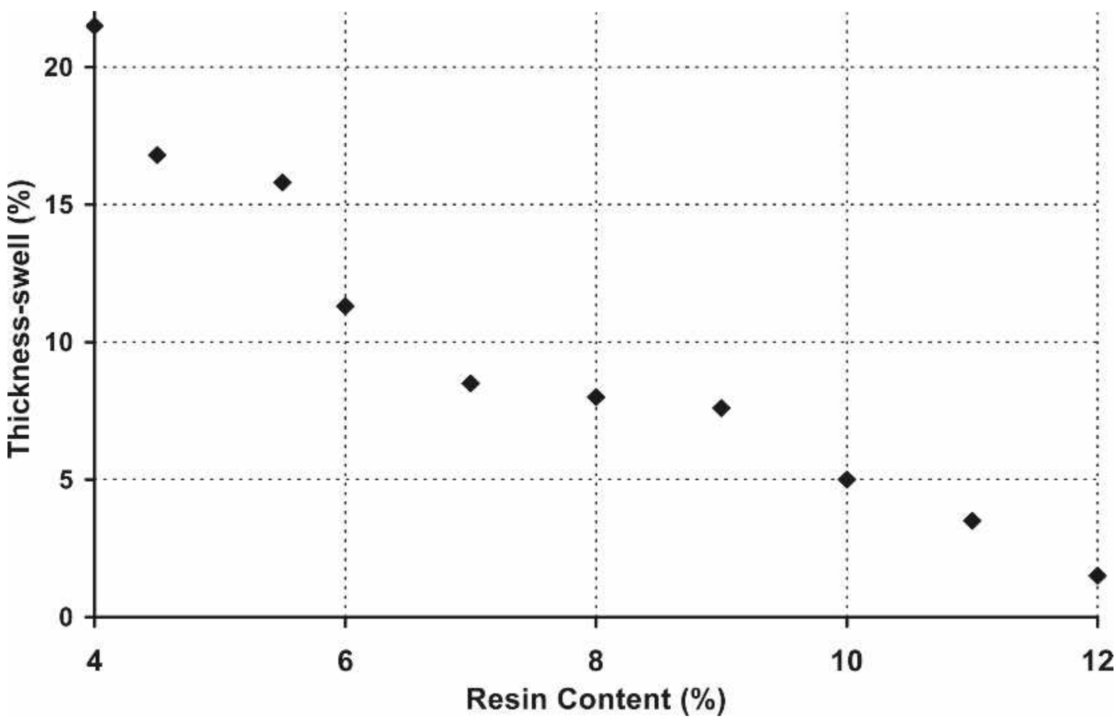

FIGURE 9. Thickness-swell vs resin content.

ing exceeded the ultimate bond strength. The rate of bond failures in the edges in nodal-plane 4, where the edge is defined as the outer 25 mm of the specimen, decreased 81–74–64% as the resin content increased 2–4–6%, respectively. In most cases, low stress levels were found in the early stages of moisture loading. As the moisture loading increased, the stresses also increased. Observations made of layer stresses in specimen 1 also showed increases as moisture loading increased. However, edge failure was less than 50%, which is lower than any of the failure rates reported for specimen 2. From Eq (1), higher resin content alone elevates the ultimate nodal strength and consequently reduces the failure rate.

CONCLUSIONS

The FE method is a powerful tool for analyzing the behavior of OSB. A recently developed FE model that accounts for the moisture transport and the nonlinear behavior through-the-thickness, was used to investigate thickness-swell, density changes, and internal stress in OSB during a soak test. The input to the model is simply the 3-D density distribution. The model enables the prediction of OSB behavior without extensive experimental tests. The model also enables the internal thickness swell, density changes, and stresses to be obtained. The use of the model is illustrated by quantifying the effects of resin content changes on thickness swell, and the examination of internal stresses and bond failures in an OSB specimen.

ACKNOWLEDGMENTS

The authors would like to thank Chris Helton and Cheng Qingzheng for their helpful assistance. The authors would also like to thank Dr. Shelton Shi of the Forestry and Wildlife Resource Center at Mississippi State University for his contribution in the acquisition of X-ray attenuation data used in the 3-D density matrix formulation.

REFERENCES

ASTM (2006) Standard test methods for evaluating properties of wood-base fiber and particle panel materials. D1037–06. American Society of Testing and Materials, West Conshohocken, PA.

Brochmann J, Edwardson C, Shmulsky R (2002) Influence of resin type and flakeboard thickness on properties of OSB. Forest Prod J 54(3):51–55.

Cloutier A, Gendron G, Blanchet P, Ganev S, Beauregard R (2001) Finite element modeling of dimensional stability in layered wood composites. Pages 63–72 *in* Proc 35th Inter Particleboard Composite Materials Symp, April 2–5, 2001, Washington State University, Pullman, WA.

Gu H, Wang S, Neimsuwan T, Wang SG (2005) Comparison study of commercial OSB flooring products in thickness swell and mechanical performance. Forest Prod J 55(12):239–245.

Linville JD (2000) The influence of a horizontal density distribution on moisture-related mechanical degradation of oriented strand composites. MS Thesis, Washington State University, Pullman, WA. 121 pp.

Suchsland O (1962) The density distribution of flakeboards. Michigan Agriculture Experiment Station. Quarterly Bulletin 45(1):104–121.

Tackie AD (2006) Determination of oriented strandboard properties from a 3D density distribution using the finite element method. PhD dissertation, The University of Tennessee, Knoxville, TN, Pp. 39–44.

———, Wang S, Bennett RM, Shi H (2008) Investigation of OSB thickness-swell based on a 3D density distribution:
Part I–The finite element model. Wood Fiber Sci 40(1): 91–102.

Van Houts J, Wang S, Shi H, Pan H, Kabalka GW (2004) Moisture movement and thickness swelling in oriented strandboard. Part. 1. Analysis using nuclear magnetic resonance microimaging. Wood Sci Technol 38(8):617–628.

———, ———, ———, Kabalka GW (2006) Moisture movement and thickness swelling in oriented strandboard. Part. 2. Analysis using a nuclear magnetic resonance imaging body scanner. Wood Sci Technol 40(6): 437–443.

Wang S, Winistorfer PM (2000) Fundamentals of vertical density profile formation in wood composites. Part 2. Methodology of vertical density formation under dynamic condition. Wood Fiber Sci 32(2):220–238.

———, ——— (2003) An optical technique for determination of layer thickness-swell of MDF and OSB. Forest Prod J 53(9):64–71.

Wu Q, Lee M (2002) Thickness swelling of oriented strandboard under long-term cyclic humidity exposure condition. Wood Fiber Sci 34(1):125–139.

Zhang Y, Jin J, Wang S (2007) Effects of resin and wax on water uptake behavior of wood strands. Wood Fiber Sci 39(2):271–278.